

Simultaneous lidar and EOS MLS measurements, and modeling, of a rare polar ozone filament event over Mauna Loa Observatory, Hawaii.

Thierry Leblanc¹, Om Prakash Tripathi¹, I. Stuart McDermid¹, Lucien Froidevaux², N. J. Livesey², W. G. Read², and J. W. Waters²

Abstract. In mid-March 2005, a rare lower stratospheric polar vortex filamentation event was observed simultaneously by the JPL lidar at Mauna Loa Observatory, Hawaii, and by the EOS MLS onboard the Aura satellite. The event coincided with the beginning of the spring 2005 final warming. On March 16, the filament was observed by lidar around 0600 UT between 415 K and 455 K, and by MLS six hours earlier. It was seen on both the lidar and MLS profiles as a layer of enhanced ozone, peaking at 1.7 ppmv in a region where the climatological values are usually around or below 1 ppmv. Ozone profiles measured by lidar and MLS were compared to profiles from the Chemical Transport Model MIMOSA-CHIM. The agreement between lidar, MLS, and the model is excellent considering the difference in the sampling techniques. MLS was also able to identify the filament at another location north of Hawaii.

1. Introduction

An important source of variability in the winter and spring lower stratosphere is caused by Rossby wave fluctuations. For large amplitude waves, the winter polar vortex can stretch significantly and produce filamentary structures that propagate away from the polar regions into the mid-latitudes and occasionally break away from the vortex to mix rapidly into the mid-latitudes [Waugh *et al.*, 1994]. This type of event has been considered one of the possible causes of mid-latitude ozone decrease [e.g., Stolarski *et al.*, 1992]. On March 16, 2005 the northern polar vortex stretched exceptionally producing a large filament that propagated from Alaska southward to 19°N over the Hawaiian Islands. This stretching event was part of the early-development stage of the spring 2005 major final warming. It was captured on March 16 between 0600 and 0900 UT by the Jet Propulsion Laboratory (JPL) lidar located at Mauna Loa Observatory, HI (MLO, 19.5°N), and by the EOS MLS onboard the Aura satellite at two separate locations (20°N, and 37°N) along the first suborbital track of March 16. In this paper we will show results from the lidar and satellite measurements of the filament over Hawaii and compare them to the results of the high resolution, three-dimensional chemistry-transport model MIMOSA-CHIM. After brief descriptions of the lidar, EOS MLS, and MIMOSA-CHIM (section 2), ozone mixing ratios from all three datasets are compared (section 3). We focus on the first hours of March 16 when the filament was stretching meridionally from Alaska to Hawaii. A detailed case study of the event, including the full chemical history inside the filament, is presented elsewhere [Tripathi *et al.*, submitted to *J. Geophys. Res.*, 2006].

2. Brief description of the MLO Lidar, EOS MLS and MIMOSA-CHIM

The MLO differential absorption ozone lidar was developed by the JPL lidar group in the early 1990s in order to provide long-term measurements of stratospheric ozone at near-tropical latitudes [McDermid *et al.*, 1995]. Two-hour integration ozone profiles are routinely obtained four to five times per week with a typical 300-m to 1-km vertical resolution and a total error not exceeding 10% in the lower stratosphere. The 10-year dataset has been used to validate many instruments onboard satellite platforms, (e.g., UARS, ENVISAT, and Aura).

The Aura spacecraft was launched on July 15, 2004 into a near polar, sun-synchronous orbit with a period of approximately 100 minutes [Schoeberl *et al.*, IEEE, 2006]. The EOS MLS uses heterodyne radiometers to measure thermal emission from the limb in various spectrally-broad regions [Waters *et al.*, JAS 1999]. Vertical profiles are retrieved every 165 km along the suborbital track, covering all latitudes from 82°S to 82°N. The standard ozone product is retrieved from the 240 GHz radiometer data with a vertical resolution of 3-4 km and a precision of 0.05-0.2 ppmv in the lower stratosphere. Preliminary validation shows agreement with other stratospheric datasets at the few to 10% level [Froidevaux *et al.*, 2006].

The Modèle Isentrope du transport Méso-échelle de l'Ozone Stratosphérique par Advection (MIMOSA) was originally developed at Service d'Aéronomie du CNRS to capture and quantify the filamentary structures passing over Europe in winter and spring to assess the importance of such structures in the irreversible transport of polar air into mid-latitudes. Using global analyses or forecasted isentropic winds interpolated onto an azimuthal equidistant projection grid with a very fine resolution, potential vorticity is advected isentropically with a 1-hour elementary time-step and re-interpolated onto a regular longitude-latitude fine grid. The chemistry-extended version, called MIMOSA-CHIM, combines the PV advection scheme and the chemistry scheme of the model REPROBUS (Reactive

¹Table Mountain Facility, Jet Propulsion Laboratory, California Institute of Technology Wrightwood, CA 92397-0367

²Jet Propulsion Laboratory, California Institute of Technology, Pasadena, CA 91109

Processes Ruling the Ozone Budget in the Stratosphere). A complete description of MIMOSA-CHIM can be found in *Hauchecorne et al.* [2002], *Lefèvre et al.* [1994], and *Marchand et al.* [2003].

3. The March 16, 2005 polar filament observed by lidar and MLS, and simulated by MIMOSA-CHIM

On March 12, 2005, the northern hemisphere polar vortex, as modeled by MIMOSA, experienced a severe stretching episode on isentropic surfaces between 415 K and 455 K just west of Alaska. By March 16, the resulting filament extended southward from Alaska to the Hawaiian Islands (20°N latitude). Ozone mixing ratios output from MIMOSA-CHIM on March 16 at 00Z on the 435 K isentropic surface are shown in **Figure 1** together with the corresponding MLS ozone mixing ratios measured along the instrument's suborbital track. A time coincidence of +/-

1 hour was chosen here, which corresponds to the very first MLS suborbital track of March 16. Only the part of this orbit between 00:06 UT, when MLS was looking over the Pacific Ocean south of Hawaii, and 00:53 UT, when MLS was looking over Central Africa, will be used in the rest of this paper. The contour color scale (MIMOSA-CHIM ozone) and the symbols color scale (MLS ozone) are identical. Best agreement is reached when symbols cannot be distinguished from the contours. Despite a few areas of disagreement, MIMOSA-CHIM and MLS ozone agree remarkably well. In particular, the polar filament stretching from Alaska to Hawaii is well captured by MLS. Quantitatively, mixing ratio values of about 2 ppmv in the center of the filament near Hawaii are found for both MLS and the model. Values measured by MLS farther north of Hawaii (i.e., as the suborbital track intersects the filament near 37°N) are slightly below that of the model.

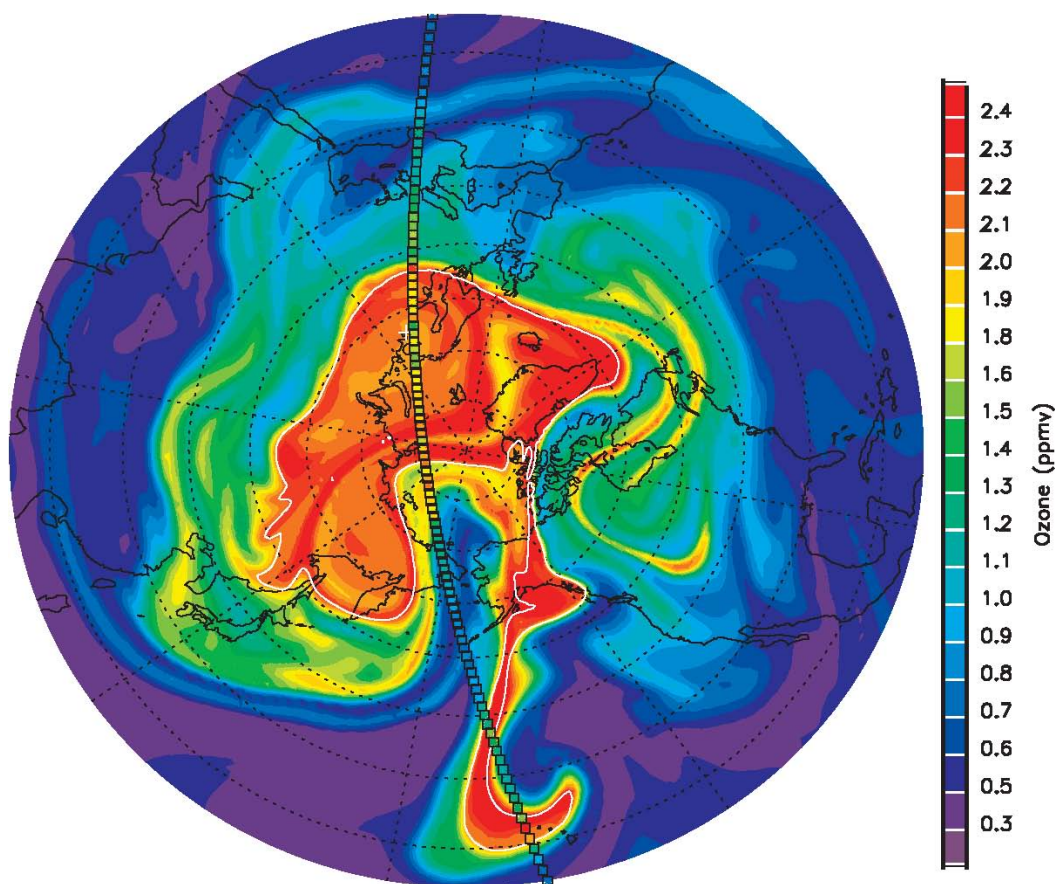


Figure 1. Ozone modeled by MIMOSA-CHIM on March 16, 2005 at 00Z on the 435 K isentropic surface, and MLS +/- 1 hour coincident ozone measurements along its suborbital track. Color scales are identical for both MLS and MIMOSA-CHIM

Ozone measured at 435 K along the MLS suborbital track is plotted in **Figure 2** (solid curve). The mixing ratio value measured by lidar at 0700 UT and 435 K is represented by an asterisk. Reactive and passive ozone modeled by MIMOSA-CHIM at 0000 UT along the same track are over-plotted with a dash-dotted curve and a dotted curve respectively. Passive ozone is defined here as a tracer with initial concentrations identical to those of ozone before the winter started and transported

passively by the model throughout the winter. There is a very good qualitative agreement between MLS and the model. Specifically, the vortex is well identified and most importantly, the two crossings of the MLS track with the filament at 20°N and 37°N are very well captured by MLS. The regions of crossing are materialized by two consecutive peaks observed on both MLS and modeled ozone. The peaks are less sharp for MLS than for MIMOSA-CHIM, especially at 37°N, but this is to be expected considering the vertical and horizontal smoothing effect resulting

from MLS measurements and retrievals [Livesey *et al.*, 2006]. Quantitative agreement is much better for the 20°N crossing, with values of about 2 ppmv for both MLS and MIMOSA-CHIM, probably because the filament is wider at 20°N than at 37°N. The MLO lidar measurement agrees well with both the model and MLS, with a value of about 1.5 ppmv, consistent with values found at the edge of the filament. A value of 2 ppmv was not measured by lidar because the center of the filament passed over MLO during daytime when no lidar measurement was possible. Nevertheless, the 1.5 ppmv lidar value is well above the typical tropical/subtropical values of 1 ppmv or less. Note that the reactive ozone concentration in the filament, as modeled by MIMOSA-CHIM, on March 16 is about half that of the model tracer. Most of the difference (1.5 ppmv) is caused by polar depletion due to halogen chemistry throughout the winter [e.g., Manney *et al.*, 2006], and the remaining part (0.5 ppmv) is due to residual tracer build-up before the winter started. A detailed study of the parcels' chemical history within the filament is provided by Tripathi *et al.* [J. Geophys. Res., 2006, submitted]. Considering the good agreement between MLS, lidar, and modeled reactive ozone, there is little doubt that the air mass above MLO on the night of March 16 was ozone-depleted from the polar region.

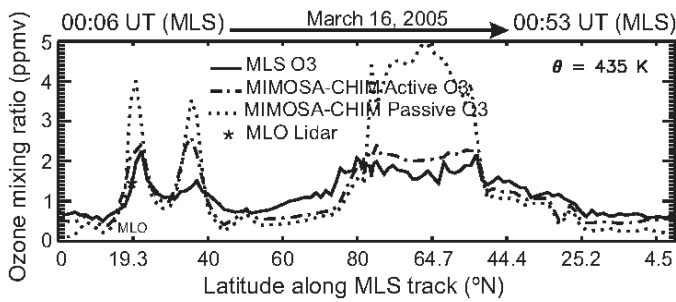


Figure 2. MLS ozone measurement at 435 K along its suborbital track (solid curve), and co-located reactive and passive ozone modeled by MIMOSA-CHIM at 00Z. The MLO lidar measurement at 06Z is represented by an asterisk symbol. See text for more details

4. Vertical structure of the filament

Figure 3 shows five selected MLS ozone profiles along the measurement track (dash), together with the corresponding MIMOSA-CHIM profiles (dotted), and with the MLO lidar profile measured at 0600 UT on March 16 (solid). The layer of enhanced ozone extends vertically from 410 K to 460 K, peaking around 435 K. The width and shape of the peak is different, depending on the measuring/modeling technique and the position along the track. The lidar profile shows the narrowest peak, which is not surprising considering its high vertical resolution in the lower stratosphere, and the observed variability of the peak throughout the measurement [Tripathi *et al.*, J. Geophys. Res., 2006, submitted]. The peak altitude measured by lidar varied by 5-10 K over the course of the night. A wider peak was observed for the MLS profiles, probably for the smoothing reasons mentioned in paragraph 3. The positions along the track were chosen to coincide with air alternately inside (blue and orange) and outside (purple, cyan, and red) the filament. The pattern out-in-out-in-out is well reproduced for both MLS and MIMOSA-CHIM.

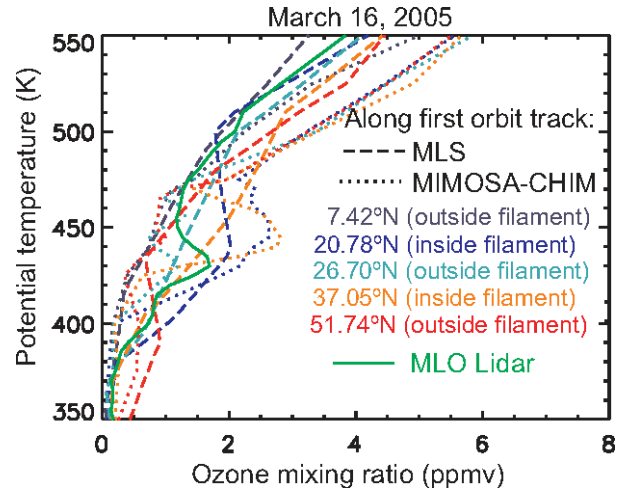


Figure 3. Ozone profiles measured on March 16 by MLS (dash curves), and calculated by MIMOSA-CHIM (dotted curves) at 4 selected locations along the suborbital track. The MLO lidar profile on the same night is over-plotted with a green solid curve

Finally in **Figure 4** we show a latitude-altitude 2D cross-section of ozone measured by MLS along its suborbital track (top), and the corresponding MIMOSA-CHIM ozone output (bottom). The two crossings with the filament are indicated by white arrows. Qualitative and quantitative agreement is very good between 400 and 500 K. The two crossings with the filament are easily identified, as is the vortex (enhanced ozone at the edges, and depleted ozone in the core). Note that ozone is overestimated by MIMOSA-CHIM at all levels above 500 K; one possible reason being too poor vertical resolution for levels above 450 K. The only apparent discrepancy between MLS and MIMOSA-CHIM in the 400-500 K range is in the filament's vertical shape and extent. The filament is seen by MIMOSA-CHIM at 37°N as a tilted structure (southward-downward tilt), while it is seen by MLS as a purely vertical disturbance. A misrepresentation of the filament by the model above 475 K, and a two-dimensional smearing effect due to the MLS smoothing procedure are possible causes for the difference.

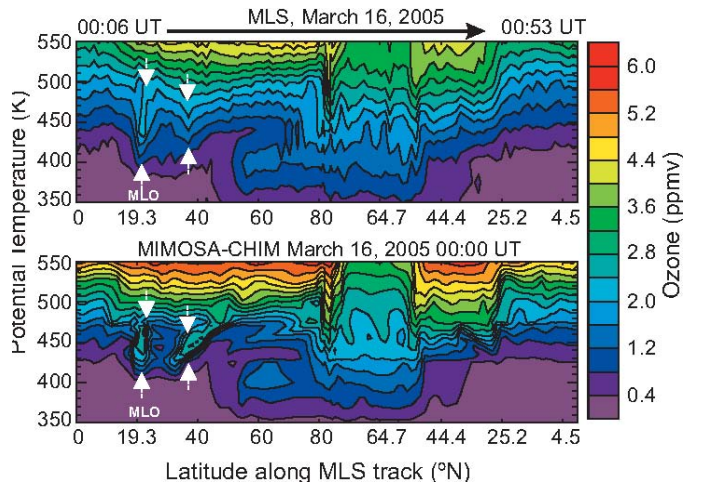


Figure 4. 2D time-altitude cross-section of MLS ozone along the suborbital track (top), and co-located reactive ozone modeled by MIMOSA-CHIM at 00Z (bottom). The position of the

crossings of the MLS track with the filament is indicated by white arrows. See text for details

4. Summary

On March 16, 2005, a rare stratospheric polar filament event was captured simultaneously by the JPL lidar located at Mauna Loa Observatory, Hawaii, and the EOS MLS instrument onboard Aura. The lidar and MLS ozone measurements were compared to the ozone outputs of the high-resolution model MIMOSA-CHIM. Excellent agreement was found both qualitatively and quantitatively between all three datasets. MLS ozone measurements not only agreed well with lidar and model between 400 K and 500 K, but MLS was also able to capture thin structures such as filaments. The filament studied here was vertically centered at 435 K, and caused ozone mixing ratios to peak at 1.5-2 ppmv in a region (20°N) where the climatological values are typically 0.5-1 ppmv. Despite its vertical resolution of about 3 km, EOS MLS seems to be a promising instrument to validate future high-resolution modeling studies. This is also confirmed by a study of vortex lamina in the 2004/2005 winter [Schoeberl *et al.*, *J. Geophys. Res.*, 2006, submitted]. Furthermore the results presented here are based, for the modeling part, on advecting a quasi-passive tracer (ozone) on isentropic surfaces, which can facilitate a global comparison of MLS measurements with ground based instruments (such as lidars and ozonesondes) using the so-called trajectory hunting technique [Danilin *et al.*, 2002] on a timescale of a few days.

Acknowledgements:

The work described in this paper was carried out at the Jet Propulsion Laboratory, California Institute of Technology, under an agreement with the National Aeronautics and Space Administration. The authors would like to thank Dr. Rob Aspey, who assisted in the collection of the lidar data used here, and Drs. Franck Lefèvre, M. Marchand, and A. Hauchecorne, who provided the original code of MIMOSA-CHIM used at JPL. MIMOSA-CHIM was run using the ECMWF T106 analyses made available for NDACC participants at the Norwegian Institute for Air Research (NILU), Norway. We thank the MLS team for producing the MLS data used here.

References

Danilin, M.Y., *et al.* (2002), Trajectory hunting as an effective technique to validate multiplatform measurements: Analysis of the MLS, HALOE, SAGE-II, ILAS, and POAM-II data in October-November 1996, *J. Geophys. Res.* 107, 10.1029/2001JD002012.

Froidevaux, L., *et al.* (2006), Early validation analyses of atmospheric profiles from EOS MLS on the Aura satellite, *IEEE Trans. Geosci. Remote Sensing*, in press.

Hauchecorne, A., S. Godin, M. Marchand, B. Heese, and C. Souprayen (2002), Quantification of the transport of chemical constituents from the polar vortex to midlatitudes in the lower stratosphere using the high-resolution advection model MIMOSA and effective diffusivity, *J. Geophys. Res.*, 107 (D20), 8289, doi: 10.1029/2001JD000491.

Lefèvre, F., G.P. Brasseur, I. Folkins, A.K. Smith, and P. Simon (1994), Chemistry of the 1991/1992 stratospheric winter: Three dimensional model simulation, *J. Geophys. Res.*, 99, 8183-8195.

Livesey, N.J., W.V. Snyder, W.G. Read, and P.A. Wagner (2006), Retrieval algorithms for the EOS Microwave Limb Sounder (MLS) instrument, *IEEE Trans. Geosci. Remote Sensing*, in press

Manney, G.L., M.L. Santee, L. Froidevaux, K. Hoppel, N.J. Livesey, J.W. Waters (2006), EOS MLS observations of ozone loss in the 2004-2005 Arctic winter, *Geophys. Res. Lett.*, in press.

Marchand, M., S. Godin, A. Hauchecorne, F. Lefevre, S. Bekki, and M. Chipperfield (2003), Influence of polar ozone loss on northern mid-latitudes regions estimated by a high-resolution chemistry transport model during winter 1999-2000, *J. Geophys. Res.*, 108(D5), 8326, doi:10.1029/2001JD000906.

McDermid, I. S., T. D. Walsh, A. Deslis, and M. L. White (1995), Optical-systems design for a stratospheric lidar system, *Appl. Opt.*, 34, 6201-6210.

Schoeberl, M.R., A.R. Douglass, E. Hilsenrath, P.K. Bhartia, J. Barnett, R. Beer, J. Waters, M. Gunson, L. Froidevaux, J. Gille, P.F. Levelt, P. DeCola (2006), Overview of the EOS Aura Mission, *IEEE Trans. Geosci. Remote Sensing*, in press.

Stolarski, R.S., R. Bajkov, L. Bishop, C. Zerefos, J. Staehelin, and J. Zawodny (1992), Measured trend in stratospheric ozone, *Science*, 256, 342-349.

Waters, J.W., *et al.* (2006), The Earth Observing System Microwave Limb Sounder (EOS MLS) on the Aura satellite, *IEEE Trans. Geosci. Remote Sensing*, in press.

Waters, J.W., *et al.* (1999), The UARS and EOS Microwave Limb Sounder Experiments, *J. Atmos. Sci.*, 56, 194-218.

Waugh, D.W., *et al.* (1994), Transport out of the lower stratosphere Arctic vortex by Rossby wave breaking, *J. Geophys. Res.*, 99, 1071-1088.